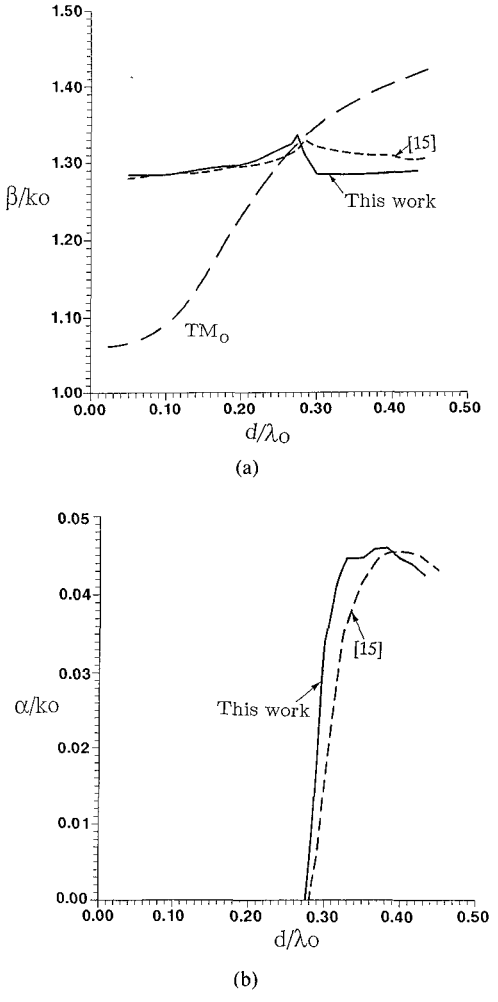

Fig. 4. Propagation constant γ for the odd conductor-backed coplanar strip mode. Referring to Fig. 1, $\epsilon_r = 2.25$, $w1/sp = w2/sp = 0.66$, $d/sp = 2.66$, $h2 = 0$, and $h1/sp = 10.66$; (a) gives β (and the propagation constant of the TM_0 parallel plate mode) and (b) gives α. A comparison is made between results computed using the method in this paper and with results computed previously using a mode matching analysis [7].

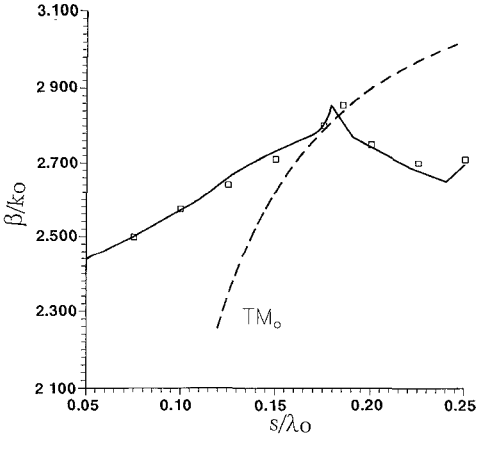

Fig. 5. Real part β of the propagation constant for coplanar strip transmission line. Referring to Fig. 1, $\epsilon_r = 10.5$, $w1/sp$ $w2/sp = 0.5$, $d/sp = 2.5$, and $h1/sp = h2/sp = 5$. The solid line represents the results of this work and the points represent the results of [2].

asymptotic procedure is accurate for expansion and testing functions separated by as few as 0.1 λ_o.

Acknowledgment

The author would like to express his gratitude to A. A. Oliner of Polytechnic University for several stimulating discussions on leaky waves and for providing the mode matching data in Fig. 4.

References

[1] L. Carin and K. J. Webb, "Isolation effects in single- and dual-plane VLSI interconnects," *IEEE Trans. Microwave Theory Tech.*, vol. 38, pp. 396-404, Apr. 1990.
[2] D. S. Phatak, N. K. Das, and A. P. Defonzo, "Dispersion characteristics of optically excited coplanar striplines: Comprehensive full wave analysis," *IEEE Trans. Microwave Theory Tech.*, vol 38, Nov. 1990.
[3] D. M. Pozar, "Input impedance and mutual coupling of rectangular microstrip antennas," *IEEE Trans. Antennas and Propagat.*, vol. AP-30, pp. 1191-1196, Nov. 1982.
[4] K. A. Michalski and D. Zheng, "Electromagnetic scattering and radiation by surfaces of arbitrary shape in a layered media, Part 1: Theory," *IEEE Trans. Antennas Propagat.*, vol. 38, pp. 335-344, Mar. 1990.
[5] M. Marin, S. Barkeshli, and P. H. Pathak, "Efficient analysis of planar microstrip geometries using a closed-form asymptotic representation of the grounded dielectric slab Green's function," *IEEE Trans. Microwave Theory Tech.*, vol. 37, pp. 669-679, Apr. 1989.
[6] K. A. Michalski, "On the efficient evaluation of integrals arising in the Sommerfeld halfspace problem," *Proc. IEEE*, vol. 132, pt. H, pp. 312-318, Aug. 1985.
[7] H. Shigesawa, M. Tsuji, and A. A. Oliner, private communication.

The Behavior of the Electromagnetic Field at Edges of Media with Finite Conductivity

Jochen Geisel, Karl-Heinz Muth, and Wolfgang Heinrich

***Abstract*—The principal behavior of both electric and magnetic fields at the edges of media with finite conductivity is investigated. We find that, as in the case of ideal conductors, the normal electric field shows a singularity at the edge. The magnetic field components, however, remain bounded if the permeabilities of the neighboring media do not differ. Detailed results on typical geometries are given.**

I. Introduction

It is well-known that singular points of the electric and the magnetic fields may occur at edges (e.g., [1], [2]). This is important, for instance, when checking the validity of surface integrals. Moreover, one can incorporate the order of singularity explicitly into numerical descriptions, which leads to very efficient modeling tools (e.g.: The basis functions used in the common spectral-domain approaches).

For the case of perfectly conducting media, detailed results are reported in the literature (see [1], [2]). Fig. 1 shows the corresponding geometry and the notation used here. A cylindrical coordinate system is used. We consider the equivalent 2-dimensional

Manuscript received January 24, 1991; revised July 22, 1991.
The authors are with the Institut fur Hochfrequenztechnik, Technische Hochschule Darmstadt, Merckstrasse 25, W-6100 Darmstadt, Germany.
IEEE Log Number 9103900.

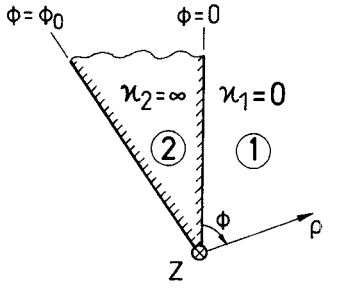

Fig. 1. Edge of a perfectly conducting medium with cylindrical geometry

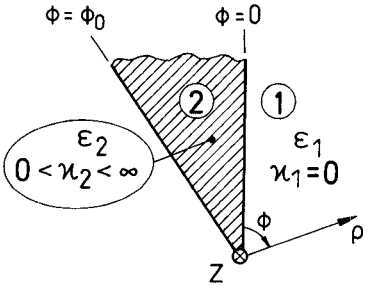

Fig. 2. The problem under investigation: edge of a conducting medium with $0 < \kappa_2 < \infty$ (otherwise identical to Fig. 1).

problem assuming homogeneity in z direction. Then the E and H field components at the edge $\rho \to 0$ behave as follows:

$$E_\rho, E_\phi, H_\rho, H_\phi \begin{cases} \sim \rho^{(\pi/\phi_0 - 1)} & \text{for } \phi_0 > \pi \text{ (unbounded)} \\ < \infty & \text{otherwise (bounded)} \end{cases}$$
$$E_z, H_z < \infty \text{ (bounded)}. \quad (1)$$

Note that in any case a bounded term in the fields may exist and thus (1) provides an explicit ρ dependence at the edge only for a singular behavior (i.e., for $\phi_0 > \pi$). This explains also the finding of a "constant term" in [3].

No general treatment, however, is available for edges of conductive media with $\kappa < \infty$. Such results are of particular importance when studying planar geometries with rectangular nonideal conductors as done, for instance, in MMIC transmission-line analysis. Recently, several approaches were reported in the literature on that subject taking into account the metallic strips as media of finite conductivity (e.g., [4]–[8]).

In reality, of course, all fields need to be bounded on physical reasons. But then, beside the finite conductivity, also no ideally sharp edges exist. One, therefore, cannot conclude from that simple consideration whether the "intermediate" case of an ideally sharp edge of finite conductivity produces singularities or not. A more detailed treatment is necessary which is presented in this paper.

II. Method of Analysis

Our analysis is based on Meixner's paper [1]. His mathematical considerations are extended here in order to cover also the case of finite conductivity values. The configuration under investigation is shown in Fig. 2. A structure homogeneous along z is assumed consisting of two neighbored isotropic media of zero and finite conductivity, respectively.

According to the cylindrical geometry the singular field behavior for $\rho \to 0$ can be described by that of the Bessel function divided by ρ. As can be seen from the Bessel-function series expansion, one has a field singularity of the form

$$\lim_{\rho \to 0} \left[\frac{1}{\rho} \cdot J_\nu(K\rho) \right] = \frac{1}{\rho} \cdot \frac{1}{\Gamma(\nu + 1)} \cdot \left(\frac{K\rho}{2} \right)^\nu \sim \rho^{\nu - 1}. \quad (2)$$

J_ν denotes the Bessel function of order ν, Γ the Gamma function, and K the separation constant. Note that in the lossy case ν assumes complex values.

Extracting the factor $\rho^{\nu - 1}$ the remainder is bounded and can be expanded in a Taylor series with respect to ρ. Thus each field component can be expressed in the following form:

$$\rho^{\nu - 1} \cdot \{a_0 + a_1 \cdot \rho + a_2 \cdot \rho^2 + \cdots\}, \qquad a_i = f(\phi, z) \quad (3)$$

with the Taylor coefficients a_i being functions of both ϕ and z as indicated. Generally, all six field components are represented by a series according to (3) but with different sets of coefficients a_i. Applying Maxwellian equations and fulfilling the continuity conditions at $\phi = 0$ and $\phi = \phi_0$ and $\phi = \phi_0 - 2\pi$, respectively, one derives a system of differential equations in ϕ for the a_i (see [1]). Nontrivial solutions can be obtained only for special values of ν. Since our aim is to determine solely the order of singularity, only those values ν_i are required for the further considerations.

Substituting ν_i back into the field components one finds the order of singularity for $\rho \to 0$: $E_\rho, E_\phi, H_\rho, H_\phi \sim \rho^{\nu_i - 1}$. The longitudinal fields E_z and H_z, on the other hand, remain bounded and their value cannot be determined solely by the edge geometry.

The range of Real(ν) is restricted to the interval]0, 1] on general reasons: Real(ν) > 0 must hold because otherwise the energy stored in the neighborhood of the edge would become infinite ("edge condition"). On the other hand, if Real(ν) > 1, the fields remain bounded, the leading term $\rho^{\nu - 1}$ in (3) becomes zero at $\rho = 0$, and hence the approach of (3) fails.

After some mathematical operations the differential system of equations separates into two decoupled algebraic problems for E_ρ, E_ϕ, and H_ρ, H_ϕ, respectively. For the geometry of Fig. 2 and the E-field case, one has the following complex-valued equation for ν:

$$\frac{\epsilon_1 - \epsilon_2}{\epsilon_1 + \epsilon_2} = + \frac{\sin(\nu_E \pi)}{\sin(\nu_E[\pi - \phi_0])} \quad (4)$$

with $\epsilon_1 = \epsilon_{r1}\epsilon_0$ and $\epsilon_2 = \epsilon_{r2}\epsilon_0 - j\kappa_2/\omega$ (see Fig. 2). Note that E_ρ and E_ϕ behave $\sim \rho^{\nu_E - 1}$.

Correspondingly, one derives for H_ρ and H_ϕ:

$$\frac{\mu_1 - \mu_2}{\mu_1 + \mu_2} = + \frac{\sin(\nu_H \pi)}{\sin(\nu_H[\pi - \phi_0])} \quad (5)$$

with $H_\rho, H_\phi \sim \rho^{\nu_H - 1}$. Note that the negative sign appears in front of the right-hand side of (4), (5) when interchanging the numbering of the lossy and the lossless region compared to Fig. 2.

In the case $\epsilon_1 = \epsilon_2$, all the electric fields remain bounded and there is no explicit dependence on the edge geometry. The same statement holds for the magnetic fields if $\mu_1 = \mu_2$.

Chow *et al.* [9] found numerically that for a rectangular strip conductor the fields for $\kappa = \infty$ and $\kappa < \infty$, respectively, differ at the edge itself but are of comparable magnitude at some distance apart. It would be interesting, therefore, to determine that critical distance range in which significant deviations occur. Such an analysis, however, cannot be formulated in a general way as presented above, because the field behavior at $\rho > 0$ depends not only on the edge geometry itself but also on the surrounding structure. Therefore, statements can be deduced only for the specific line geometry under investigation.

III. Discussion

A. Electric Field

Equations (4) and (5) show that the tangential E field components become singular only if $\epsilon_1 \neq \epsilon_2$. Particularly, in the case of a metallic conductor with $\kappa_2 \gg \omega\epsilon_0$ (4) reads

$$\frac{\epsilon_1 - \epsilon_2}{\epsilon_1 + \epsilon_2} \approx -1 + 2j\epsilon_{r1} \cdot \frac{\omega\epsilon_0}{\kappa_2} + 2\epsilon_{r1}(\epsilon_{r1} + \epsilon_{r2}) \cdot \left(\frac{\omega\epsilon_0}{\kappa_2}\right)^2 = \frac{\sin(\nu_E \pi)}{\sin(\nu_E[\pi - \phi_0])}. \tag{6}$$

In the microwave range and for realistic metallic conductivity values the term $\omega\epsilon_0/\kappa_2$ is very small (lower than 10^{-6}). Therefore, the E-field singularity should approximate the value $\nu_E = \pi/\phi_0$ for $\kappa = \infty$ (see (1)). Our numerical investigations confirmed this observation. For that purpose, we employed a perturbation approach which gives the deviation of ν_E from the $\kappa = \infty$ value $\nu_{E\infty} = \pi/\phi_0$. For the structures of interest the difference $|\nu_E - \nu_{E\infty}|$ ranges in the order below 10^{-12} and thus one may use the value $\nu_{E\infty}$ with excellent accuracy.

That statement, of course, does not hold if one considers an infinitely thin layer ($\phi_0 = 2\pi$). Then one finds $\nu_E - 1 = -1/2$ for $\kappa = \infty$ (field singularity $\sim \rho^{-1/2}$), whereas $\nu_E - 1 = 0$ (bounded fields) is obtained for $\kappa < \infty$. In the latter case, namely, region (2) in Fig. 2 has zero thickness and thus does not disturb the fields at all.

B. Magnetic Field

For $\mu_1 = \mu_2$, in contrast to the electric field, the H components remain bounded independent of the conductivity value as far as $\kappa_2 < \infty$ holds. As a consequence, the limit $\kappa_2 \to \infty$ differs from the $\kappa_2 = \infty$ value. A noncontinuous transition takes place. Only if media with different permeabilities are involved H_ρ and H_ϕ become singular $\sim \rho^{\nu_H - 1}$ at the edge according to (5).

One further consideration supports the result for $\mu_1 = \mu_2$ and $\kappa_2 < \infty$: As well known, in the dc limit $f \to 0$ the current density inside a nonideal conductor becomes uniformly distributed and, consequently, the H field has to remain bounded (see [10]).

C. Three-Region Problem

In the presence of two dielectric and one conductive regions as depicted by Fig. 3, a similar mathematical procedure as described in Section II may be applied (see [2]). After some lengthy operations, again two decoupled conditions for ν_E and ν_H can be deduced.

Regarding the singularities, the results correspond to those of the two-region problem treated before, except for one special aspect: Both in the lossy and the lossless case for certain parameter constellations (i.e.: ϕ_1 small and ϕ_2 slightly larger than π, depending also on $\epsilon_{r1}/\epsilon_{r2}$), all fields remain bounded. Regarding the analysis of planar transmission lines, however, that observation has no practical relevance.

IV. Conclusions

We will confine our considerations to the planar transmission-line geometries found in microwave circuits and MMIC's. Owing to the rectangular conductor cross-sections, for this class of problems primarily the 90-degree angle is of importance. Fig. 4 illustrates such a geometry. It describes, for example, the case of a conductor edge located at the top of a dielectric substrate.

For that configuration, the tangential E field components are singular at the edge with approximately the same order as in the corresponding geometry with $\kappa_3 = \infty$. The tangential H field components, on the other hand, become bounded and thus the transition between $\kappa_3 \to \infty$ and $\kappa_3 = \infty$ is not continuous. That means, for instance: It is not justified to assume the tangential magnetic fields at the edge to be approximately equal in both cases. Thus one concludes that any perturbational approach based on that approximation fails if the influence of the fields at the edge is predominant.

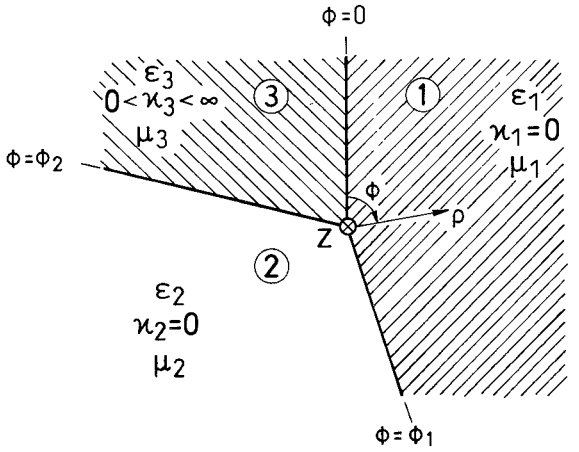

Fig. 3. The three-region problem: edge of a conducting medium with $0 < \kappa_3 < \infty$ neighbored by two dielectric regions.

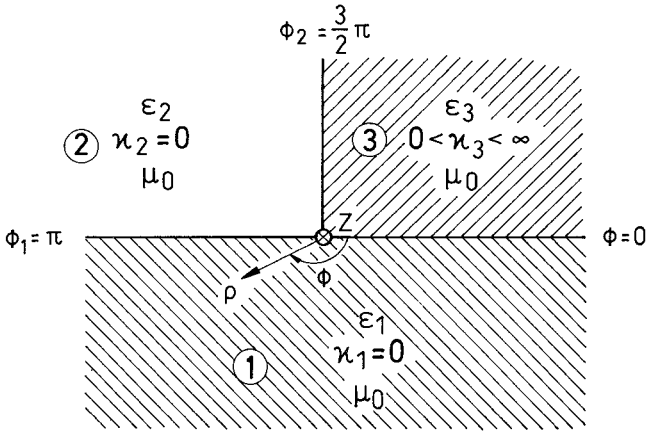

Fig. 4. Typical geometry found in microwave transmission-line analysis: rectangular conductor at the top of a dielectric substrate ($\mu_i = \mu_0$, the notation refers to Fig. 3).

More precisely, the results can be summarized as follows (the notation refers to Fig. 4):

	$\kappa_3 = \infty$	$\kappa_3 < \infty$
E_ρ, E_ϕ	$\sim \rho^{\nu_E - 1} \to \infty$	$\sim \rho^{\nu_E' - 1} \to \infty$
H_ρ, H_ϕ	$\sim \rho^{(\pi/\phi_0) - 1} \to \infty$	bounded
E_z, H_z	bounded	bounded

(7)

with $\nu_E' \approx \nu_E$ and

$$\begin{cases} \nu_E = \dfrac{\pi}{\phi_0} & \text{for } \epsilon_{r1} = \epsilon_{r2} \\ \dfrac{\epsilon_{r1} - \epsilon_{r2}}{\epsilon_{r1} + \epsilon_{r2}} = \dfrac{\sin(\nu_E \pi)}{\sin(\nu_E[\pi - \phi_0])} & \text{otherwise} \end{cases} \tag{8}$$

Assuming $\epsilon_{r1}/\epsilon_{r2} > 2$, for instance, one finds $0.5 < \nu_E < 0.6$, which is similar to the case of an infinitely thin strip in an homogeneous medium ($\nu_E = 0.5$).

ACKNOWLEDGMENT

The authors are grateful to Prof. H. L. Hartnagel for his continuous support and encouragement.

REFERENCES

[1] J. Meixner, "The behavior of electromagnetic fields at edges," *IEEE Trans. Antennas Propagat.*, vol. AP-20, pp. 442–446, July 1972.
[2] R. Mittra and S. W. Lee, *Analytical Techniques in the Theory of Guided Waves*. New York: Macmillan, 1971, sec. 1.3.
[3] A. S. Omar and K. F. Schünemann, "Application of the generalized spectral-domain technique to the analysis of rectangular waveguides with rectangular and circular inserts," *IEEE Trans. Microwave Theory Tech.*, vol. 39, pp. 944–952, June 1991.
[4] W. Heinrich, "Full-wave analysis of conductor losses on MMIC transmission-lines," *IEEE Trans. Microwave Theory Tech.*, vol. 38, pp. 1468–1472, Oct. 1990.
[5] S. T. Peng, C. K. C. Tzuang, and Chu-Dong Chen, "Full-wave analysis of lossy transmission line incorporating the metal modes," *1990 IEEE MTT-S Int. Microwave Symp. Dig.*, Dallas, TX, vol. 1, pp. 171–174.
[6] R. Faraji-Dana and Y. L. Chow, "The current distribution and a.c. resistance of a microstrip structure," *IEEE Trans. Microwave Theory Tech.*, vol. 38, pp. 1268–1277, Sept. 1990.
[7] F. J. Schmückle and R. Pregla, "The method of lines for the analysis of lossy planar waveguides," *IEEE Trans. Microwave Theory Tech.*, vol. 38, pp. 1473–1479, Oct. 1990.
[8] W. Schröder and I. Wolff, "Full-wave analysis of normal- and superconducting transmission lines by hybrid-mode boundary integral equation method," in *1991 IEEE MTT-S Int. Microwave Symp. Dig.*, Boston, MA, vol. 1, pp. 341–344.
[9] R. Faraji-Dana and Y. Chow, "Edge condition of the field and ac resistance of a rectangular strip conductor," *IEEE Proc*, vol. 137, pt. H, pp. 133–140, Apr. 1990.
[10] W. Heinrich, "Conductor losses and their influence on circuit performance in planar MMIC's," in *Proc. Workshop F, 1991 MTT-S IEEE Int. Microwave Symposium*, Boston, MA.

Experimental Wide-Stopband Filters Utilizing Asymmetric Ferrite Junctions

H. How, Y. Liu, S. Zhang, C. Vittoria, C. Carosella, and V. Folen

***Abstract*—Filters incorporating asymmetric stripline Y-junction circulators have been fabricated and tested over the frequency range of 0.05 to 18 GHz. The passband frequency was near 2 GHz. The insertion loss was ~2 dB and the stopband extended from 4.5 to 18 GHz with transmission ≤ −30 dB. The filter includes ferrite discs in which high order modes have been eliminated as calculated in an earlier paper [2].**

INTRODUCTION

Filter designs incorporating ferrite materials have been developed for the past 25 years. Typically a polished sphere of single crystal YIG is fed through two orthogonal semi-circular wire loops such that the two wires become tightly coupled at the ferrimagnetic resonant frequency of the YIG sphere [1]. However, this design is susceptible to magnetostatic mode excitations above and below the main ferrimagnetic resonance mode. In addition, instabilities of the spin waves can induce the excitation of other subsidiary resonance modes. Altogether, excitations of these extraneous modes give rise to spurious transmissions at frequencies off the fundamental passband frequency. The power handling capacity in a resonant device is therefore quite low (~100 mW). In a previous paper [2] we investigated the feasibility of constructing a ferrite filter utilizing a Y-junction circulator design. By careful design of the junction geometry high order modes of excitations can be effectively suppressed and, hence, the stopband transmission of the device can be extended many times the fundamental frequency. Since wide stopband filters are currently needed for radome applications, we find here an example of ferrite devices that can be utilized to protect electronic components in high-power and/or high-noise environments. For a typical stripline circulator operating below 30 GHz the CW power handling capability can be as high as several hundred watts [3], since non-resonant properties of the ferrite are utilized in the microwave transmission mechanism.

A circulator is defined as a three-port device arranged such that the energy entering a port is coupled to an adjacent port but not to the third port. A circulator requires its three ports to be arranged symmetrically with respect to one another. However, one may relax this 3-fold symmetry to obtain one more degree of freedom in designing a circulator filter. Strictly speaking, this asymmetric design cannot be referred to as a circulator design and, therefore, we call our device a circulator design only under a restricted basis. In [2] we have established the circulation conditions for an asymmetric circulator, which determined in turn the radius of the ferrite disc and the dielectric ratio of the ferrite and the dielectric filling material [2].

In this paper we report our experimental work following the design conditions predicted by the theory [2]. We have fabricated several asymmetric circulators using three different kinds of ferrite materials. Experimentally, we find that transmissions due to high order mode excitations have been effectively suppressed and the reflection and transmission characteristics compare reasonably well with our calculations [2]. Using two circulators in cascade we measure 2.1 dB insertion loss, 33 dB isolation, and the stopband extending more than two octaves of the transmission frequency.

EXPERIMENTS

Fig. 1 depicts the geometry of an asymmetric circulator where the three ports are designated as the input, output, and isolated ports. The angle θ denotes half the asymmetric port separation angle (not necessarily equal to 60°), and ψ is half the suspension angle of the three ports. As predicted in [2] a circulator filter design can be realized by assigning the two angles θ and ψ both equal to 45°. Furthermore, the theory also predicts the following values:

$$\omega_o/\omega_m = 2.1, \quad \omega_f/\omega_m = 2.0, \quad \gamma\Delta H/\omega_m = 0.012,$$
$$\mu = 6.12, \quad \kappa = 4.88, \quad \mu_{\text{eff}} = 2.23,$$
$$\epsilon_d/\epsilon_f = 0.092, \quad x = 0.157, \quad z = 4.92,$$

where μ and κ are the Polder tensor elements defined by

$$\mu = 1 + \frac{\omega_m\omega_o}{\omega_o^2 - \omega^2}, \quad \kappa = \frac{\omega_m\omega}{\omega_o^2 - \omega^2},$$

Manuscript received January 25, 1991, revised July 18, 1991. This work was supported by ONR and the Naval Research Laboratory.

H. How, Y. Liu, S. Zhang, and C. Vittoria are with the Electrical and Computer Engineering Department, Northeastern University, Boston, MA 02115.

C. Carosella and V. Folen are with the Naval Research Laboratory, Washington, DC 20375.

IEEE Log Number 9103903.